4.1.2

BUCKLING TESTS ON ECCENTRICALLY LOADED BEAM COLUMNS

By J. Cassens

NATIONAL ADVISORY COMMITTEE FOR AERONAUTICS

TECHNICAL MEMORANDUM NO. 989

BUCKLING TESTS ON ECCENTRICALLY LOADED BEAM COLUMNS*

By J. Cassens

Formulas are obtained for computing the buckling load of rods eccentrically loaded at each end, the computation being extended in particular to the inelastic range. The test results are graphically presented on three sets of curves. Two of these, at least for the elastic range, are independent of the material tested. The third set (see charts 3a and 3b), which is independent of the material, possesses greater clearness and is therefore used for comparing the test results with the theoretical. On chart 6 a comparison is made between the buckling load of an eccentrically loaded open profile and the torsional buckling load of the same profile centrally loaded. For large slenderness ratios the eccentrically loaded rod can sustain a greater load in the axial direction.

NOTATION

f (cm^2) cross-sectional area of rod

a (cm) distance of outer fibers, with stress σ_o, from neutral axis

J (cm^4) moment of inertia, $J = i^2 f$

i (cm) radius of gyration

W (cm^3) resistance moment

e (cm) eccentricity (fig. 1)

u, l (cm) see fig. 1

$\lambda = l/i$ slenderness ratio of rod

δ_m (cm) deflection at center of rod

v (cm) deflection of neutral axis, $v = f(u)$

E (kg/cm^2) elasticity modulus

T (kg/cm^2) buckling modulus, according to Engesser

P   (kg)   axial load

M   (cm kg)   moment, a function of the axial load P

P_{Br} (kg)   axial load in failure

P_E (kg)   buckling load: $P_E = \pi^2 f T/\lambda^2$

P_{E_0} (kg)   Euler load: $P_{E_0} = \pi^2 f E/\lambda^2$

$$\xi = \frac{P_E}{P}$$

$$x = \frac{e\,a}{i^2}$$

$$y = \frac{B_{Br}}{P_E} = \frac{\sigma_{Br}}{\sigma_E}, \quad y_0 = \frac{\sigma_{Br}}{\sigma_{E_0}}$$

$$c = \frac{\sigma_0}{\sigma_E} = \frac{\sigma_0 \lambda^2}{\pi^2 T}, \quad c_0 = \frac{\sigma_0}{\sigma_{E_0}}$$

σ (kg/cm^2) stress

σ_0 (kg/cm^2) stress in outer fibers in failure from
                bending and axial load

σ_E (kg/cm^2) buckling stress: $\sigma_E = \pi^2 T/\lambda^2$

σ_{E_0} (kg/cm^2) buckling stress of Euler load: $\sigma_{E_0} = \pi^2 E/\lambda^2$

σ_g (kg/cm^2) limiting stress for which the Euler formula
                ceases to be valid

σ_{Br} (kg/cm^2) axial stress at center of gravity during
                failure

σ_e (kg/cm^2) bending stress (fig. 2)

1. INTRODUCTION

There are several problems in connection with eccentrically loaded beam columns, for which a theoretical solution is as yet unavailable. Although the problem may be theoretically formulated, it is necessary to rely on tests for an explanation and final solution. Two such problems are the following:

1. In eccentrically loaded beam columns, what importance should be assigned to the buckling modulus?

2. For which total stress $P/f + M(P)/W$ is the beam no longer able to support any increased load?

For the purpose of answering these questions the Focke-Wulf firm has undertaken a number of tests on beams loaded as shown in figure 1.

2. COMPUTATIONAL FORMULAS

The beam deflection was computed on the principle of "passive work."[*] The deflection at the center δ_m is obtained from the computation of the passive work $1 \, \delta_m$ performed by the assumed load "1" – this load acting at the location in the direction of the required deflection – when the actual load P is applied to the beam. From the known relation there is obtained:

$$1 \, \delta_m = 2 \int_0^{l/2} \frac{(P \, c + P \, v)(\tfrac{1}{2} u)}{E \, J} \, du$$

$$\delta_m = P \, c \, \frac{l^2}{8 \, EJ} + \int_0^{l/2} \frac{P \, v \, u}{E \, J} \, du$$

---

[*]The term is explained in greater detail in the author's paper "Tafel einiger Knick-Biege-Fälle," which will appear shortly.

For the deflection v, we assume an expression which satisfies the boundary conditions for $u = 0$; $u = l/2$ and $u = l$:

$$v = \delta_m \sin\left(\pi \frac{u}{l}\right)$$

There is then obtained:

$$\delta_m \left(1 - \frac{P l^2}{\pi^2 E J}\right) = P e \frac{l^2}{8 E J}$$

The maximum bending moment acts at the center and can be computed from the following equation:

$$M_{max} = P e + P \delta_m$$

After several transformations, there is obtained for M_{max} the following expression:

$$M_{max} = P e \frac{\xi + 0.233}{\xi - 1} \tag{1}$$

The above is true on the assumption that the buckling modulus is equal to the E modulus. It will be explained below how this relation applies also in the inelastic range.

We now have an expression for the maximum stress:

$$\sigma_{max} = \frac{P}{f} + \frac{P e}{W} \frac{\xi + 0.233}{\xi - 1} \leqq \sigma_o \tag{2}$$

where σ_o can approximately be set equal to the compressive strength of the material. For thin-walled sections it is advisable to substitute for this the "collapsing" strength - by which term we may denote the longitudinal stress obtained from compression tests on short-length specimens, of slenderness ratio < 10.

An answer has thus been found to the second question in the Introduction. The theoretical answer, however, can only be confirmed by comparison with the test results.

To express the results of equation (2) in the form of a curve chart, the relation is transformed for the limiting case of maximum load so that $\sigma_{max} = \sigma_0$. There is obtained

$$x = \frac{\frac{c}{y} + y - (1 + c)}{1 + 0.233\,y} \qquad (3)$$

where

$$c = \frac{\sigma_0}{\sigma_E}; \quad y = \frac{P_{Br}}{P_E} = \frac{\sigma_{Br}}{\sigma_E}; \quad x = \frac{e\,a}{i^2}$$

3. GRAPHICAL PRESENTATION OF THE RESULTS

Chart 1 shows the graph of equation (3). The abscissa is the nondimensional ratio $x = e\,a/i^2$, which is an expression for the eccentricity. The following device was made use of in plotting. The curves were plotted for values of x from 0 to 1. For $x > 1$, the reciprocal values of x were taken and thus y as a function of $1/x$ from 1 to 0. In this way all possible values of x are included in the figure. The magnitude c_0, which includes the maximum stress, the slenderness ratio, and the E modulus or buckling modulus is taken as the parameter of the curves. The ordinate is the quotient $y_0 = P_{Br}/P_{E_0}$. This ratio is equivalent to P_{Br}/P_E, provided the longitudinal stress is small enough so that the computation with the elasticity modulus E is valid. In order to take into account also short rods of small eccentricity in which longitudinal stresses P/f may occur which exceed the stress σ_g, the rupturing load P_{Br} for these rods was also referred to the Euler load computed with the E modulus. This, in addition to computational advantages, has the following advantage for the representation of the results: If P_{Br} were referred to P_E, then all the c_0 parameter curves for $x = 0$ would end at point $y = 1$. This would mean large inaccuracies in the family of curves for small values of x and c_0.

On chart 1 is also shown the limiting curve. To the right of this curve the longitudinal stresses are so small that the buckling computation with the E modulus is absolutely justified. To the left of the limiting curve, however, the trend of the family of curves c_0 depends on the material, the position of the limiting curve itself depending on the material and to some extent on the shape of the rod cross section.

To determine the limiting curve, an assumption is made which is fundamental as regards question 1 in the Introduction. It is assumed that the longitudinal stress of the beam P/f determines whether the buckling computation is to be carried out with the E modulus or with the buckling modulus. If $P/f > \sigma_g$, then the buckling modulus corresponding to the state of stress is to be used in the computation; while for $P/f < \sigma_g$ the E modulus is to be used. The stress σ_g is thus the criterion in determining whether the E modulus or the buckling modulus is to be used.

The method is clarified in figure 2. Assume a rod is to be computed of slenderness ratio λ_1. Depending on the eccentricity, the rod can take up longitudinal stresses which are smaller or greater than σ_g, up to the failure load. If they are smaller than σ_g the E modulus is to be used. For the slenderness ratio λ_1, the limiting point is

$$\frac{\sigma_{Br}}{E_{o_1}} = \frac{\sigma_g}{E_{o_1}} = y_g = \frac{\sigma_g}{\sigma_o} c$$

where σ_g and σ_o depend mainly on the material but also on the shape of the rod. In the relation

$$y_g = \frac{\sigma_g}{\sigma_o} c \qquad (4)$$

we now have a simple expression for computing y_g as a function of c. Substituting (4) in equation (3) in order to make c approach zero, there is obtained:

$$x = \frac{\Delta\sigma}{\sigma_g} \frac{1 - y_g}{1 + 0.233 \, y_g} \qquad (4a)$$

or, solving for y_g

$$y_g = \frac{\dfrac{\Delta\sigma}{\sigma_g} - x}{\dfrac{\Delta\sigma}{\sigma_g} + 0.233 \, x} \qquad (4b)$$

To compute the family of curves with parameter c_0,
a) an expression for the buckling modulus is introduced in equation (3), namely:

$$T = E \frac{\sigma_0 - \sigma}{\Delta\sigma}$$

and there is thus obtained

$$x = \frac{\sigma_0/\sigma - 1 - \frac{\Delta\sigma}{\sigma_0} c_0}{1 + 0.233 \frac{\Delta\sigma}{\sigma_0} \frac{c_0}{\sigma_0/\sigma - 1}}$$

Our object, however, is to express x as a function of σ_{Br}/σ_{E_0}. Hence the expression takes the following form:

$$x = \frac{c/\bar{y} - 1 - \frac{\Delta\sigma}{\sigma_0} c_0}{1 + 0.233 \frac{\Delta\sigma}{\sigma_0} \frac{c_0}{c/\bar{y} - 1}} \qquad (5)$$

Relations (4a) and (4b) can, of course, be derived from equation (5) with the aid of (4). It should also be remarked that $c/\bar{y} = c_0/y_0$.

b) An expression for the buckling modulus according to the Tetmajer lines is introduced in equation (3), namely:

$$T = \frac{\sigma}{\pi^2} \left(\frac{\sigma_0 - \sigma}{\Delta\sigma/\lambda_g} \right)^2$$

There is then obtained the following expression for the family of c_0 parameter curves to the left of the limiting curve:

$$x = \frac{\sigma_0/\sigma - 1 - \frac{\Delta\sigma^2 \sigma_g}{(\sigma_0 - \sigma) \sigma_{E_0} \sigma}}{1 + 0.233 \frac{\Delta\sigma^2 \sigma_g}{(\sigma_0 - \sigma)^2 \sigma_{E_0}}}$$

Again transforming the above so that x is a function of σ_{Br}/σ_{E_o}, there is obtained

$$x = \frac{(c/y - 1) - \dfrac{\Delta\sigma^2 \; \sigma_g}{\sigma_o^3} \dfrac{c_o \; (c/y)^2}{(c/y - 1)}}{1 + 0.233 \dfrac{\Delta\sigma^2 \; \sigma_g}{\sigma_o^3} \dfrac{c_o \; (c/y)^2}{(c/y - 1)^2}} \qquad (6)$$

In chart 2 the ordinate is the same as in chart 1, but for the abscissa there is taken the ratio $c_o = \sigma_o/\sigma_{E_o}$ with x as parameter. The limiting curve can be very simply drawn in by (4). To the right of the limiting curve the E modulus is to be used for the computation, while to the left of the curve the buckling modulus is used.

Still a third form of graphically representing the equations (3), (5), and (6) will now be shown in chart 3. It is clear that these curves can be drawn using the values for charts 1 and 2. The relations will, however, be modified to correspond to the new forms of representation. We are required to find σ_{Br} as a function of λ with x as parameter. After several transformations there is obtained the relation:

$$\lambda^2 = \frac{E \; \pi^2}{\sigma_{Br}} \; \frac{\sigma_o/\sigma_{Br} - (1 + x)}{\sigma_o/\sigma_{Br} - (1 - 0.233 \; x)} \qquad (7)$$

In the above expression the significance of the assumption as regards the use of the buckling modulus for beam-column computations is particularly well brought out. The limiting curve in this case is simply the horizontal $\sigma = \sigma_g$. Above this line relation (7) must be transformed and becomes:

a)   with the expression for the buckling modulus

$$T = E \; \frac{\sigma_o - \sigma}{\Delta\sigma}$$

$$\lambda^2 = \frac{E \; \pi^2}{\sigma_{Br}} \; \frac{\sigma_o/\sigma_{Br} - (1+x)}{\sigma_o/\sigma_{Br} - (1-0.233 \; x)} \; \frac{\sigma_o - \sigma_{Br}}{\Delta\sigma} \qquad (8)$$

b)   and with the buckling modulus according to Tetmajer, straight lines:

$$T = \frac{\sigma}{\pi^2}\left(\frac{\sigma_0 - \sigma}{\Delta\sigma}\right)^2 \lambda_g^2 = E\frac{\sigma}{\sigma_g}\left(\frac{\sigma_0 - \sigma}{\Delta\sigma}\right)^2$$

$$\lambda^2 = \frac{E\pi^2}{\sigma_{Br}}\frac{\sigma_0/\sigma_{Br} - (1+x)}{\sigma_0/\sigma_{Br} - (1-0.233\,x)}(\sigma_0/\sigma_{Br} - 1)^2\frac{\sigma_{Br}^3}{\Delta\sigma^2\sigma_g} \qquad (9)$$

By means of the family of curves with parameter x, charts 3a and 3b, the stress due to the axial loads on the rod is represented. The total stress which can be sustained by the rod in the outer fibers at the middle of its length is, according to the definition, σ_0. These relations are again presented in figure 3. For the eccentricity x the rod can take up an axial load corresponding to the stress σ_{Br}. The stress due to the bending is then σ_e.

To show more clearly the conditions on increasing the axial load, the outer fiber stress $\sigma = P/f + M(P)/W$ is plotted in figure 4 against the axial load P for various eccentricities for a steel tube of diameter 30 X 1 and of length, 100 centimeters. The dotted line gives the increase in purely axial stress with increasing axial load; that is, for eccentricity zero. The buckling load $P_E = 1890$ kilograms. It may also be seen that even if greater stresses than the Euler stresses in the outer fibers are permitted, no greater longitudinal forces than those of the Euler load can be computed. For the eccentricity of 5 centimeters there is also shown dotted the curve $P/f + M/W$ without buckling deflection. For this large eccentricity, therefore, the buckling effect is very small. It consists of the difference between the continuous and dotted curves. With decreasing eccentricity the curves approach the linear stress P/f and the limiting curve P_E.

If the end points of the family of curves for the stress of 6000 kg/cm^2, namely, the values for P_{Br} were plotted against the eccentricity, a diagram similar to chart 1 would be obtained. The example here chosen corresponds approximately to a value of $c = 3$.

4. COMPARISON OF THE THEORY WITH TEST RESULTS

With regard to the employment of the buckling modulus

and the maximum stress, the procedure now is the following:
From the tests, certain values x, c, λ, etc., are deter-
mined. In charts 4, 5, 6, only those x-parameter curves
were plotted for which tests were conducted. Charts 4 to 6
are analogous to chart 3, since the test results are most
clearly represented in this form. Comparison with the test
values provides a critique of the validity of the proposed
computation methods.

The results are typical for buckling tests, particu-
larly for small slenderness ratios. If such tests are not
conducted with laboratory accuracy there is a large scat-
tering of the results. The tests conducted cannot, however,
be considered as laboratory tests and in practice, buckling
members are not generally manufactured to laboratory pre-
cision. With regard to each of the charts 4, 5, and 6,
the following remarks may be made.

Chart 4: The points with parameter value x = 2 lie
quite well on the curve and similarly, the points with
parameter x = 1.33 and x = 1. Only for the values x =
0.5 for slenderness ratio $\lambda = 40$ is there a strong scat-
tering. Comparing, however, the values x = 0.5 for $\lambda =$
40 and $\lambda = \sim 70$, it is found that there was hardly any
increase in the failure axial load on decreasing the
length from a value corresponding to the slenderness ratio
70 to that corresponding to slenderness ratio 40. As this
result is improbable, these points should be checked anew.
The two upper points x = 0.5 and $\lambda = 40$ indicate that
the value of $\sigma_g = 3400$ kg/cm^2 has also been chosen some-
what high. The table below gives the ratio of the eccen-
tricity to the mean radius of the circular tube used in
the tests.
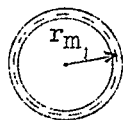
$x \rightarrow$	0.5	1	1.33	2
e/r_m	0.25	0.5	0.67	1

Chart 5: The test points lie above the theoretical
curve. They could be made to lie more closely on the
curves by taking σ_0 somewhat larger than 3800. The
curve x = 0 indicates the need for caution, however, in
assuming a higher value for σ_0.

Chart 6: This chart shows tests with C sections
connected as shown in figure 5. The test points lie well

on the theoretical curves. The buckling curve of a centrally loaded beam which is capable of being freely twisted about its shear center is also shown for comparison - the curve being taken from the work of Kappus, Jahrbuch 1937 der Deutschen Luftfahrtforschung, page I 409. It will here be seen that for the usual slenderness ratios the eccentrically loaded section can sustain a greater longitudinal load than the centrally loaded section which has a less favorable degree of freedom. The computation of the torsional buckling values is given in the appendix.

The eccentric buckling tests were extended by joining those and similar rods into a framework. In this case the buckling values of the joined rods are naturally somewhat higher. This is principally due to their being joined to the other rods under tensile load.

5. CONCLUDING REMARKS

On the basis of the test values and from comparison of these values with the theoretical curves, it may be stated that the buckling process may, with sufficient accuracy, be represented by the theory given above. Examination of the curves leads to the following observations.

It is preferable to conduct tests on eccentrically loaded rather than on centrally loaded beams. Generally great difficulty will be found in conducting buckling tests on centrally loaded beams. The difficulty consists in the fact that the buckling value of a centrally loaded beam is determined by the offset of the neutral axis at each section from the line joining the points of application of the load. The amount of this tolerance, which is not capable of being measured, is decreased by the presence of an eccentricity. In buckling tests on centrally loaded beams failure occurs due to the moment $P \Delta$ where Δ is the tolerance. In compression tests on eccentrically loaded beams, failure is due to the moment $P (e + \Delta)$. From this it may be seen that the effect of the tolerance vanishes with increasing value of e.

The tests reported in the present paper are only those conducted by Focke-Wulf. Results of other previous tests were also evaluated (Thielemann, Jahrbuch 1937 der Deutschen Luftfahrtforschung, p. I 386). The results agree almost completely with our own. One phenomenon, however,

is there brought out more clearly than in our paper. For large slenderness ratio the test points lie somewhat below the theoretical curve, while for smaller slenderness ratio they lie above - and the more so the greater the deflection due to bending (fig. 6); that is, the greater σ_e. In other words, for large slenderness ratio the stability part predominates in the failure of the beam, and for small slenderness ratio the stress part predominates and an effect arises that is called the "bending factor." (See reference 1.)

Besides the references already given there may be mentioned, from the very extensive literature on the subject, the book of Karl Jezek (reference 2). This book gives a very detailed treatment of the flow processes or what has been noted above as "bending factor" and the effect of the cross-sectional shape. The book is intended particularly for steel structural problems.

APPENDIX

Torsional Buckling of Centrally Compressed Open Sections in the Elastic Range (Reference 3)

According to equations (47), (48), (56), and (58), we have for the torsional buckling stress σ_D of a section, symmetric with respect to the x-axis:
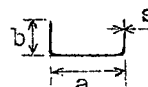
$$(I) \qquad \sigma_D = \frac{\sigma_s + \sigma_x}{2} - \sqrt{\left(\frac{\sigma_s - \sigma_x}{2}\right)^2 + \rho_x^2}$$

$$(II) \quad \begin{cases} \sigma_x = \frac{\pi^2}{l^2}\frac{E\,J_x}{F} \\[2em] \sigma_s = \dfrac{G\,J_T + \frac{\pi^2}{l^2}E\,C}{J_p} \\[2em] \rho_x = \frac{\pi^2}{l^2}\frac{E\,R_x}{\sqrt{F J_p}} \end{cases}$$

where

(II) cont. $\begin{cases}\end{cases}$

J_x moment of inertia with respect to the x-axis

J_p polar moment of inertia

J_T $\frac{1}{3} U s^3$, torsional resistamce (U = perimeter, s = thickness)

R_x $\int y\,w\,d\,F$, deformation moment for the x-axis

C $\int w^2\,d\,F - \frac{1}{F}(w\,dF)^2$, resistance to deformation about the center of gravity

w unit deformation

For a U-section, equations (I) and (II), by approximating the roots of equation (I), can be put in the form (see equations (69) to (72) in the above paper (reference 3)):

$$(III) \qquad \sigma_D = \frac{\pi^2 E}{\lambda^2}[\alpha + \beta \lambda^2]$$

$$(IV)\begin{cases} \alpha = \frac{A_1 + A_2}{2} - \sqrt{\left(\frac{A_1 - A_2}{2}\right)^2 + A_3^2} \\[3ex] \beta = \frac{B}{2}\left(1 - \frac{A_1 - A_2}{2}\right)\frac{1}{\sqrt{\left(\frac{A_1 - A_2}{2}\right)^2 + A_3^2}} \end{cases}$$

$$(V)\begin{cases} A_1 = \frac{3a^2(a + 2b)(2a^2 + 15\,ab + 26\,b^2)}{(2a + b)[a^2(a + 6b)(a + 2b) + 4b^2(2a + b)]} \\[3ex] A_2 = \frac{a^2(a + 6b)(a + 2b)}{4b^3(2a + b)} \\[3ex] A_3 = \frac{6a^2(a+2b)(a+3b)}{b(2a+b)\sqrt{3}[a^2(a+6b)(a+2b) + 4b^3(2a+b)]} \\[3ex] B = \frac{\frac{4}{\pi^2}\frac{G}{E}(a+2b)^2 s^2}{[a^2(a+6b)(a+2b) + 4b^3(2a+b)]} \end{cases}$$

In the special cases there is obtained:

$$20 \times 20 \times 0.5 \qquad \sigma_x = \frac{\pi^2 E}{\lambda^2} \left[0.18 + 0.079 \left(\frac{\lambda}{100}\right)^2 \right]$$

$$20 \times 15 \times 0.5 \qquad \sigma_p = \frac{\pi^2 E}{\lambda^2} \left[0.31 + 0.136 \left(\frac{\lambda}{100}\right)^2 \right] \qquad \lambda = \frac{l}{i_y}$$

REFERENCES

1. Cassens, J.: Einige Bemerkungen zur Gewichtsfrage, Querschnutt und Gewichtsaufwand. Z.F.M., July 1933, pp. 382 and 383.

2. Jezĕk, Karl: Die Festigkeit von Druckstäben aus Stahl. Julius Springer, Wien, 1937.

3. Kappus, Robert: Twisting Failure of Centrally Loaded Open-Section Columns in the Elastic Range. T.M. No. 851, NACA, 1938.
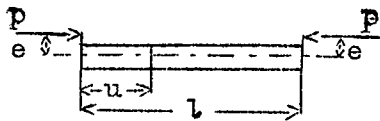
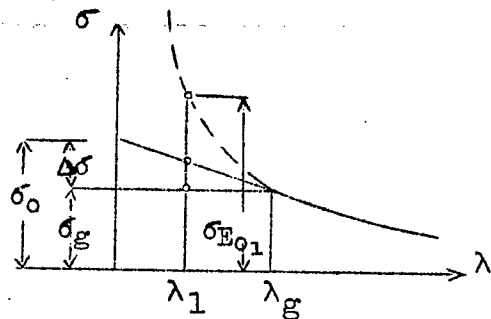Figure 1.- Eccentrically
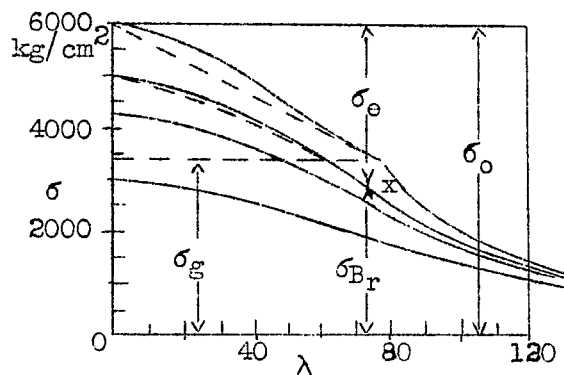loaded rod.

Figure 2.- Buckling stress
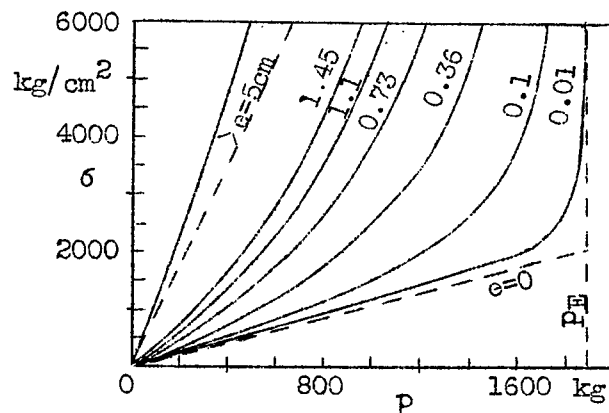diagram.

Figure 3.- Buckling and bending stresses.

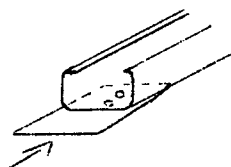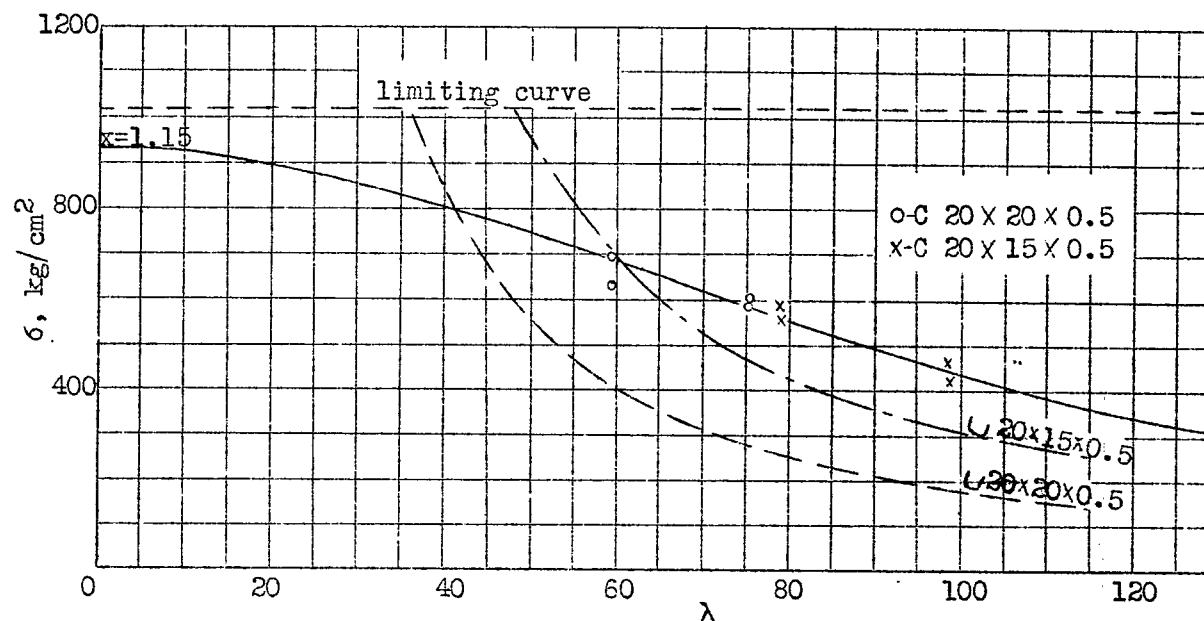Figure 4.- Stresses in steel tube 30×1 for
various eccentricities.

Figure 5.- Connection for test C section.

o-C 20 X 20 X 0.5
x-C 20 X 15 X 0.5

limiting curve

x=1.15

U 20x15x0.5

U 20x20x0.5

For comparison, torsional buckling.

Test No. 1026- C-sections 20×20×0.5 and 20×15×0.5.

$$\begin{cases} \lambda^2 = \dfrac{\pi^2 E}{\sigma_{Br}} \cdot \dfrac{\dfrac{\sigma_0}{\sigma_{Br}} - (1+x)}{\dfrac{\sigma_0}{\sigma_{Br}} - (1-0.233x)} & \begin{array}{l}\text{holds for}\\ \sigma_{Br} \leqq \sigma_g\end{array} \\[4ex] \lambda^2 = \dfrac{\pi^2 E}{\sigma_{Br}} \cdot \dfrac{\dfrac{\sigma_0}{\sigma_{Br}} - (1+x)}{\dfrac{\sigma_0}{\sigma_{Br}} - (1-0.233x)} \cdot \dfrac{\sigma_0 - \sigma_{Br}}{\Delta\sigma} & \begin{array}{l}\text{holds for}\\ \sigma_{Br} \geqq \sigma_g\end{array} \end{cases}$$

$$\begin{cases} \sigma_D = \dfrac{\pi^2 E}{\lambda^2}\left[0.18 + 0.079\left(\dfrac{\lambda}{100}\right)^2\right] \text{ for } \cup\ 20\times20\times0.5 \ \Big\}\begin{array}{l}\text{dotted}\\\text{curve}\end{array} \\[3ex] \sigma_D = \dfrac{\pi^2 E}{\lambda^2}\left[0.31 + 0.136\left(\dfrac{\lambda}{100}\right)^2\right] \text{ for } \cup\ 20\times15\times0.5 \ \Big\}\begin{array}{l}\text{dot-dash}\\\text{curve}\end{array} \end{cases}$$

$$E = 7\cdot10^5 \text{kg/cm}^2$$
$$\sigma_0 = 2000 \text{ kg/cm}^2$$
$$\sigma_g = 1020 \text{ kg/cm}^2$$

Chart 6.

$y = \dfrac{P_{Er}}{P_{Eo}}$

$x = e \cdot a / i^2$ $x = i^2 / e \cdot a$

$C_o = \dfrac{\sigma_o}{\sigma_{Eo}} = 4.0$

3.5
3.0
2.5
2.0
1.75
1.5
1.25
1.0
0.8 0.9
0.7
0.6
0.5

limiting curve

$y = \dfrac{\dfrac{\Delta\sigma}{\sigma_g} - x}{\dfrac{\Delta\sigma}{\sigma_g} + 0.233x}$

$x = \dfrac{c/y + y - (1+c)}{1 + 0.233\,y}$

limiting curve

valid to right
of limiting
curve.

$x = \dfrac{\dfrac{\sigma_o}{\sigma} - 1 - \dfrac{\Delta\sigma}{\sigma_o} \cdot c_o}{1 + 0.233 \dfrac{\Delta\sigma}{\sigma_o} \cdot \dfrac{c_o}{\sigma_o/\sigma - 1}}$ (continuous)

$x = \dfrac{(c/y - 1) - \dfrac{\Delta\sigma^2 \sigma_g}{\sigma_o^3} \dfrac{c_o (c/y)^2}{c/y - 1}}{1 + 0.233 \dfrac{\Delta\sigma^2 \sigma_g}{\sigma_o^3} \dfrac{c_o (c/y)^2}{(c/y - 1)^2}}$

valid to
left of
limiting
curve
(dotted)

$E = 2 \cdot 10^6 \, kg/cm^2$
$\sigma_o = 6000 \ kg/cm^2$
$\sigma_g = 3400 \ kg/cm^2$
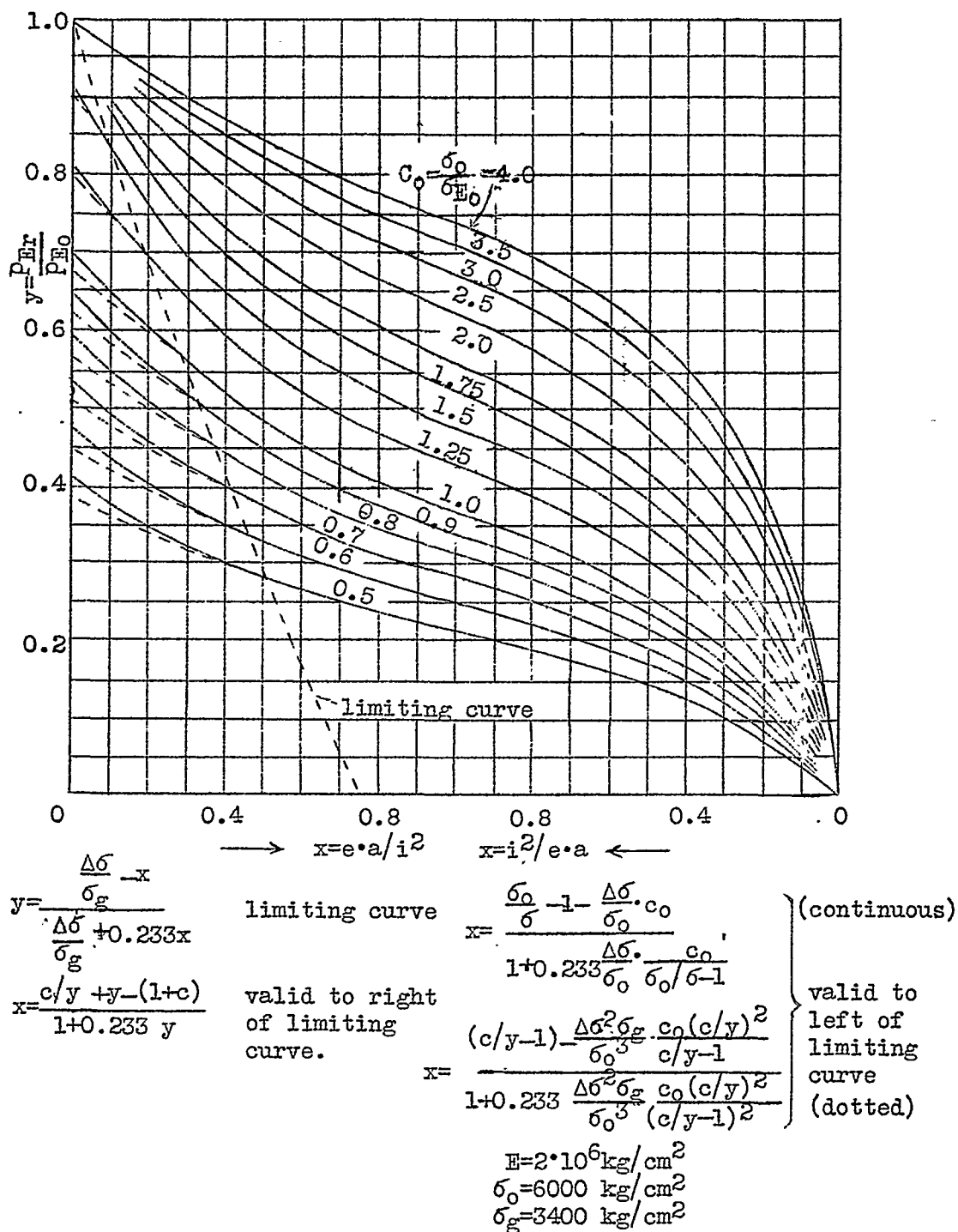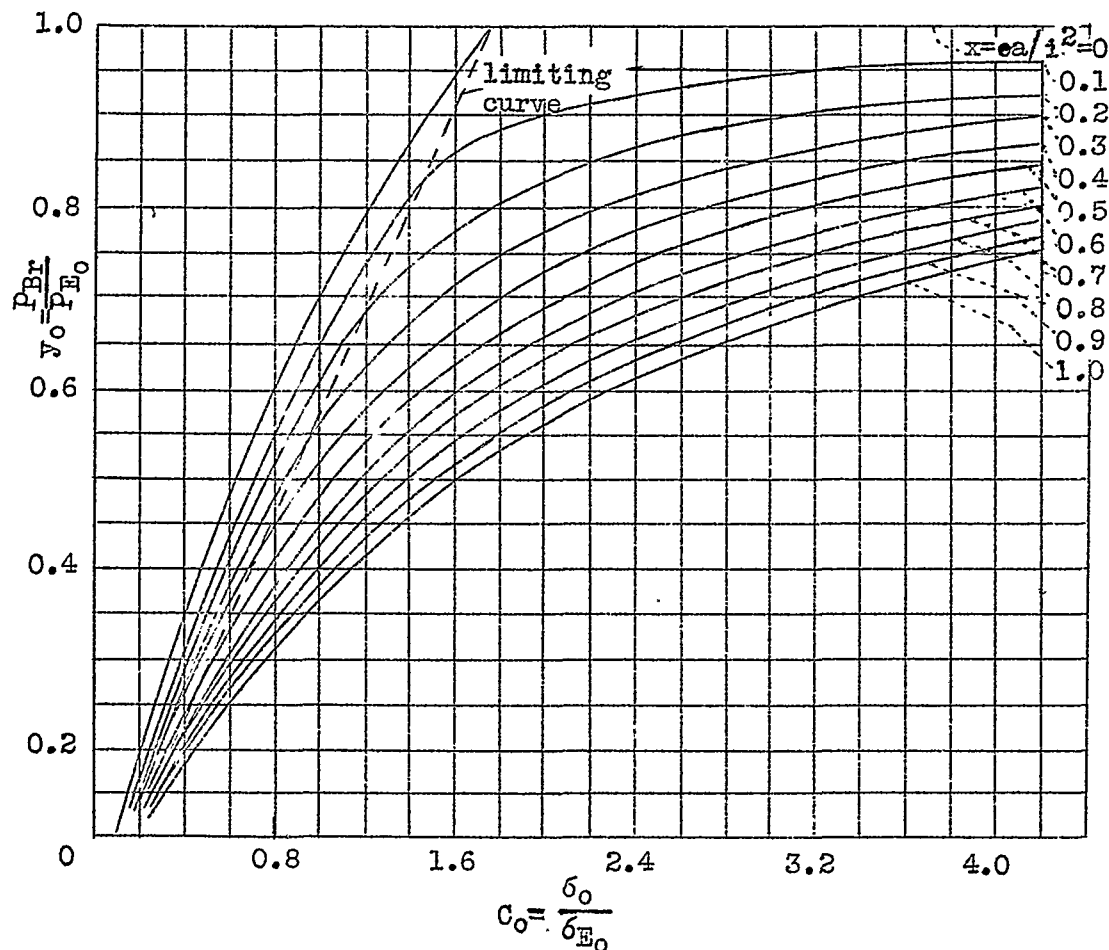
Chart 1.

$$y= \frac{\sigma_g}{\sigma_o}\cdot c \qquad \text{limiting curve}$$

$$x= \frac{c/y+y-(1+c)}{1+0.233\ y} \qquad \begin{array}{l}\text{valid to right}\\ \text{of limiting curve}\end{array}$$

$$x= \frac{\dfrac{\sigma_o}{\sigma}-1-\dfrac{\Delta\sigma}{\sigma_o}\cdot c_o}{1+0.233\dfrac{\Delta\sigma}{\sigma_o}\ \dfrac{C_o}{\sigma_o/\sigma-1}} \qquad \begin{array}{l}\text{valid to left}\\ \text{of limiting}\\ \text{curve}\end{array}$$

$$E= 2\cdot10^6 \text{kg/cm}^2$$
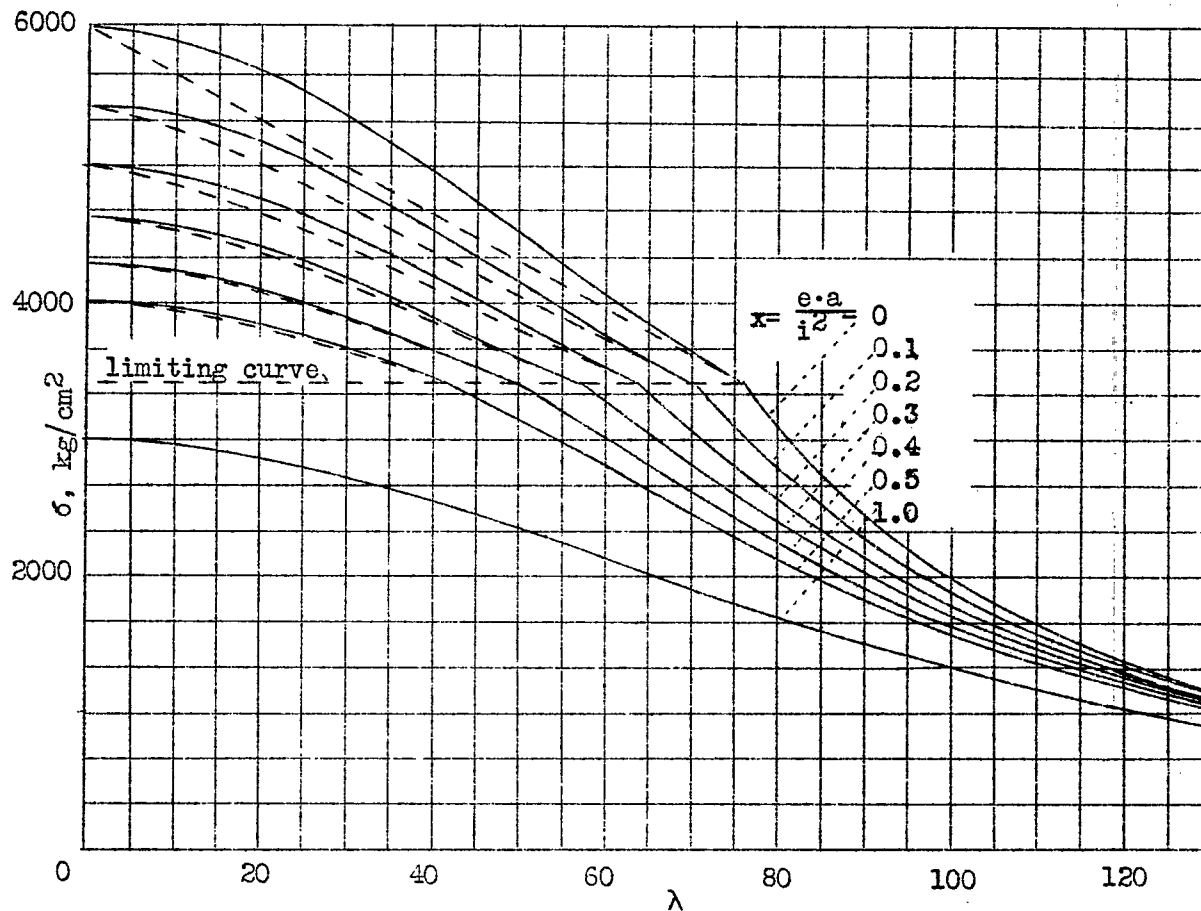$$\sigma_o= 6000 \text{ kg/cm}^2$$
$$\sigma_g= 3400 \text{ kg/cm}^2$$

Chart 2.

$\sigma = \sigma_g$　　limiting curve

$$\lambda^2 = \frac{\pi^2 E}{\sigma_{Br}} \cdot \frac{\dfrac{\sigma_0}{\sigma_{Br}} - (1+x)}{\dfrac{\sigma_0}{\sigma_{Br}} - (1-0.233x)}$$

holds for $\sigma_{Br} \lessgtr \sigma_g$

$$E = 2 \cdot 10^6 \, kg/cm^2$$
$$\sigma_0 = 6000 \; kg/cm^2$$
$$\sigma_g = 3400 \; kg/cm^2$$

limiting curve

$x = \dfrac{e \cdot a}{i^2} = 0$

0.1
0.2
0.3
0.4
0.5
1.0

σ, kg/cm^2

λ

$$\lambda^2 = \frac{\pi^2 E}{\sigma_{Br}} \cdot \frac{\dfrac{\sigma_0}{\sigma_{Br}} - (1+x)}{\dfrac{\sigma_0}{\sigma_{Br}} - (1-0.233x)} \cdot \frac{\sigma_0 - \sigma_{Br}}{\Delta\sigma}$$

(continuous)

holds for $\sigma_{Br} \gtreqless \sigma_g$

$$\lambda^2 = \frac{\pi^2 E}{\sigma_{Br}} \cdot \frac{\dfrac{\sigma_0}{\sigma_{Br}} - (1+x)}{\dfrac{\sigma_0}{\sigma_{Br}} - (1-0.233x)} \cdot \left(\frac{\sigma_0 - \sigma_{Br}}{\Delta\sigma}\right)^2 \cdot \frac{\sigma_{Br}}{\sigma_g}$$
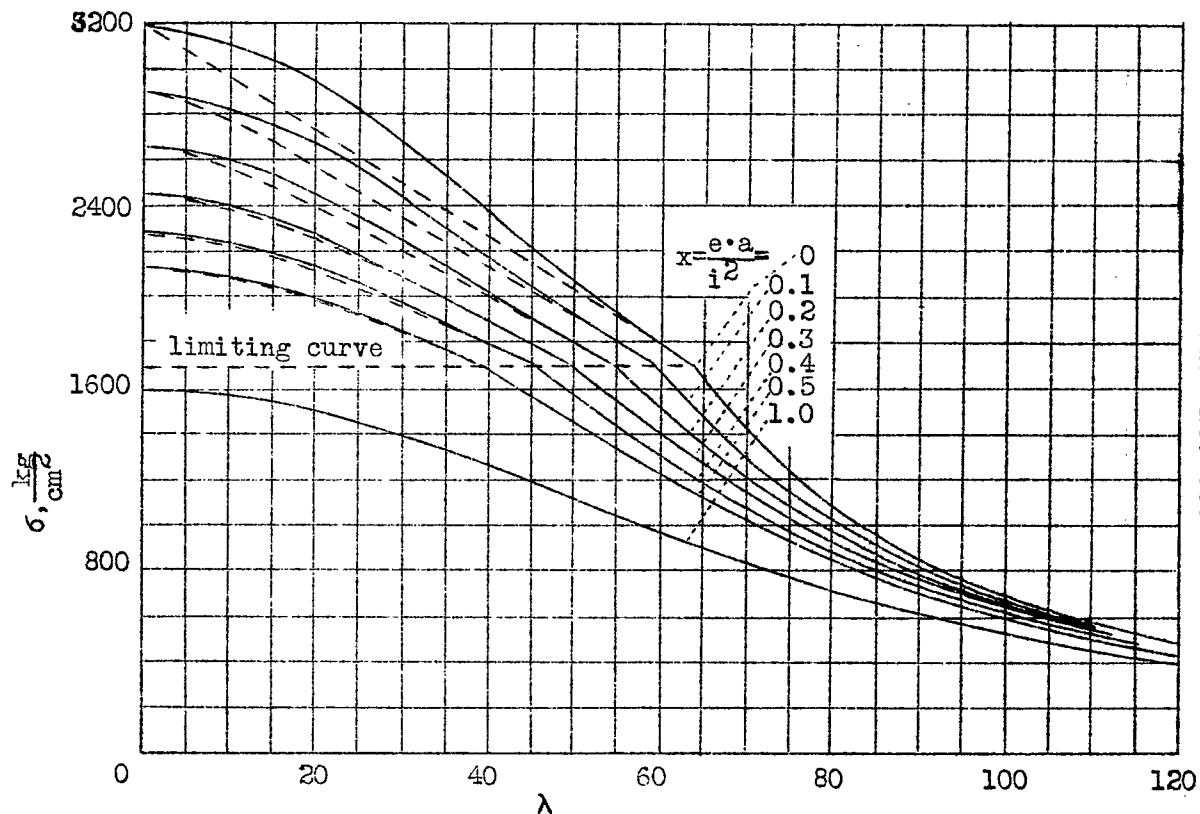
(dotted)

Chart 3a.

$\sigma = \sigma_g$ limiting curve

$$\lambda^2 = \frac{\pi^2 E}{\sigma_{Br}} \cdot \frac{\dfrac{\sigma_0}{\sigma_{Br}} - (1+x)}{\dfrac{\sigma_0}{\sigma_{Br}} - (1-0.233x)}$$
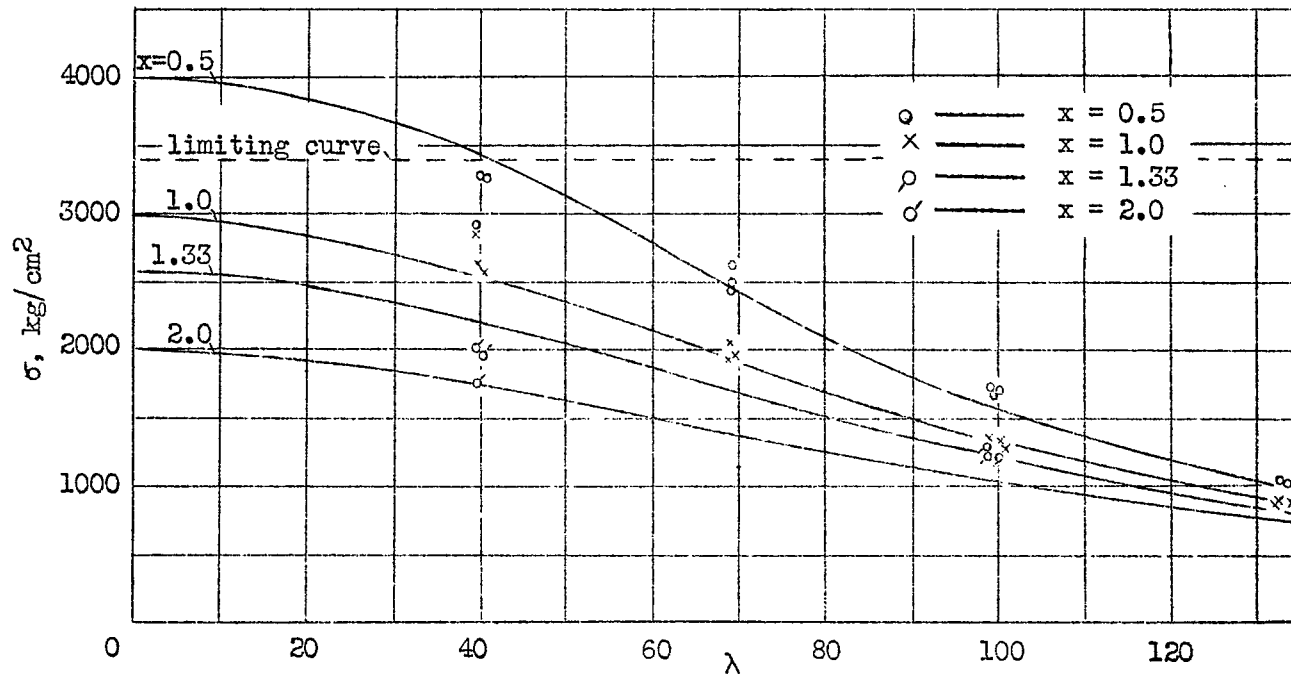
holds for $\sigma_{Br} \leqq \sigma_g$

$E = 7 \cdot 10^5 \, \text{kg/cm}^2$
$\sigma_0 = 3200 \, \text{kg/cm}^2$
$\sigma_g = 1700 \, \text{kg/cm}^2$

limiting curve

$x = \dfrac{e \cdot a}{i^2} =$ 0
0.1
0.2
0.3
0.4
0.5
1.0

$\sigma, \dfrac{kg}{cm^2}$

λ

$$\left. \lambda^2 = \frac{\pi^2 E}{\sigma_{Br}} \cdot \frac{\dfrac{\sigma_0}{\sigma_{Br}} - (1+x)}{\dfrac{\sigma_0}{\sigma_{Br}} - (1-0.233x)} \cdot \frac{\sigma_0 - \sigma_{Br}}{\Delta\sigma} \right\} \text{holds for} \left\{ \lambda^2 = \frac{\pi^2 E}{\sigma_{Br}} \cdot \frac{\dfrac{\sigma_0}{\sigma_{Br}} - (1+x)}{\dfrac{\sigma_0}{\sigma_{Br}} - (1-0.233x)} \cdot \left(\frac{\sigma_0 - \sigma_{Br}}{\Delta\sigma}\right) \cdot \frac{\sigma_{Br}}{\sigma_g} \right.$$

(continuous) $\sigma_{Br} \geqq \sigma_g$ (dotted)
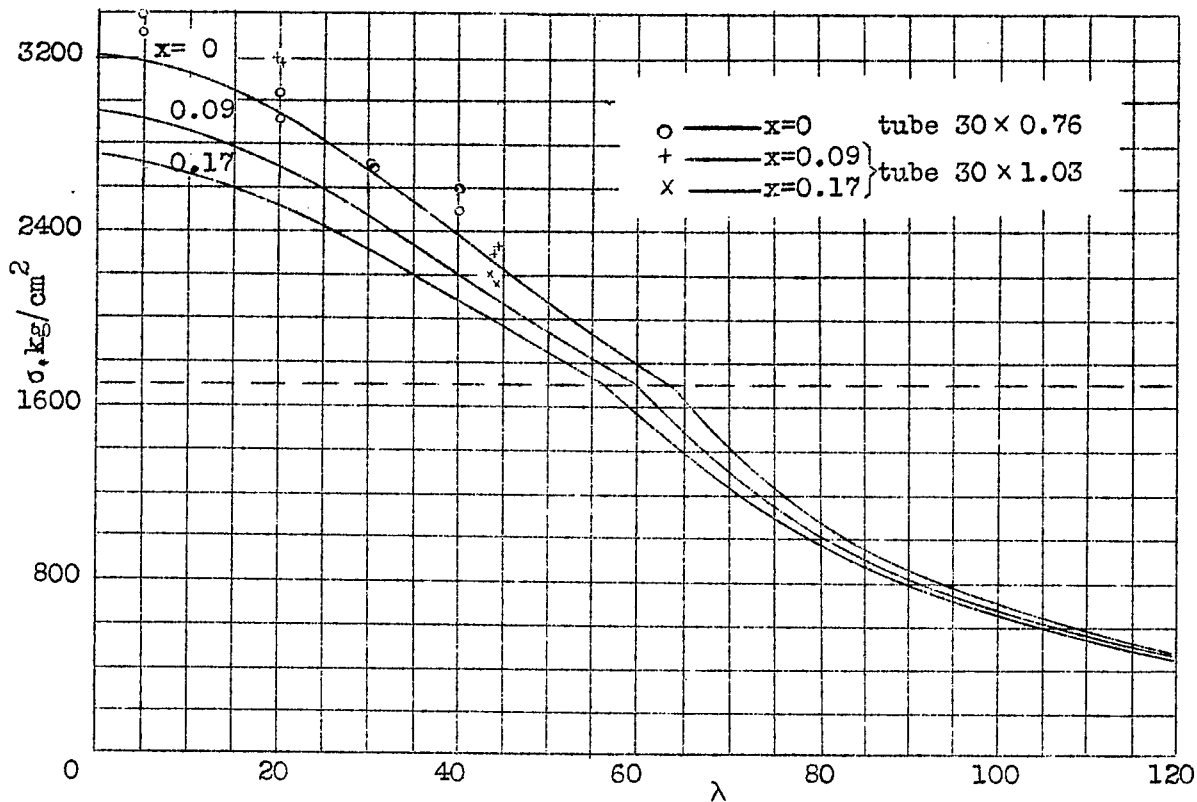
Chart 3b.

Test no. 1632 (Cr Mo 60 steel tube)

$$\lambda^2 = \frac{\pi^2 E}{\sigma_{Br}} \cdot \frac{\dfrac{\sigma_0}{\sigma_{Br}} - (1+x)}{\dfrac{\sigma_0}{\sigma_{Br}} - (1-0.233x)} \qquad \text{holds for } \sigma_{Br} \lessgtr \sigma_g$$

$$\lambda^2 = \frac{\pi^2 E}{\sigma_{Br}} \cdot \frac{\dfrac{\sigma_0}{\sigma_{Br}} - (1+x)}{\dfrac{\sigma_0}{\sigma_{Br}} - (1-0.233x)} \cdot \frac{\sigma_0 - \sigma_{Br}}{\Delta\sigma} \qquad \text{holds for } \sigma_{Br} \lessgtr \sigma_g$$

$$E = 2 \cdot 10^6 \, \text{kg/cm}^2$$
$$\sigma_0 = 6000 \, \text{kg/cm}^2$$
$$\sigma_g = 3400 \, \text{kg/cm}^2$$

Chart 4.

Chart 4.

Test no. 1786 (dural tube 30 × 0.76)
Test no. 1780 (dural tube 30 × 1.03)

$$\lambda^2 = \frac{\pi^2 E}{\sigma_{Br}} \cdot \frac{\dfrac{\sigma_0}{\sigma_{Br}} - (1+x)}{\dfrac{\sigma_0}{\sigma_{Br}} - (1-0.233x)} \qquad \text{holds for } \sigma \lessgtr \sigma_g$$

$$E = 7 \cdot 10^5 \text{kg/cm}^2$$
$$\sigma_0 = 3200 \text{ kg/cm}^2$$
$$\sigma_g = 1700 \text{ kg/cm}^2$$

$$\lambda^2 = \frac{\pi^2 E}{\sigma_{Br}} \cdot \frac{\dfrac{\sigma_0}{\sigma_{Br}} - (1+x)}{\dfrac{\sigma_0}{\sigma_{Br}} - (1-0.233x)} \cdot \frac{\sigma_0 - \sigma_{Br}}{\Delta\sigma} \qquad \text{holds for } \sigma \gtrless \sigma_g$$

Chart 5.